A versatile synthesis route for metal@SiO2 core-shell nanoparticles using 11-mercaptoundecanoic acid as primer

Zhang, Y.; Kong, X.; Xue, B.; Zeng, Q.; Liu, X.; Tu, L.; Liu, K.; Zhang, H.

DOI
10.1039/c3tc31171f

Publication date
2013

Document Version
Final published version

Published in
Journal of Materials Chemistry. C

Journal of Materials Chemistry C

RSC Publishing

PAPER

View Article Online
View Journal | View Issue

Cite this: *J. Mater. Chem. C*, 2013, **1**, 6355

A versatile synthesis route for metal@SiO_2 core–shell nanoparticles using 11-mercaptoundecanoic acid as primer†

Youlin Zhang,[ac] Xianggui Kong,*[a] Bin Xue,[ab] Qinghui Zeng,[a] Xiaomin Liu,[a] Langping Tu,[ab] Kai Liu[c] and Hong Zhang*[c]

Received 18th June 2013
Accepted 30th July 2013

DOI: 10.1039/c3tc31171f

www.rsc.org/MaterialsC

Applying the Stöber method to directly coat noble metal nanoparticles (NPs) such as gold (Au) and silver (Ag) NPs with silica shells presents challenges, since the noble metal NPs are not stable in alcoholic solution and have low chemical affinity for silica. This paper describes a method which uses 11-mercaptoundecanoic acid (MUA) as a linker molecule between the silica shell and the noble metal NPs. MUA binds strongly to the surface of the NPs *via* a metal–S bond by replacing the standard capping agents on the surface of the NPs. Upon MUA stabilization, the NPs can be transferred into alcohol solution and show chemical affinity for silica. The MUA-modified NPs can be directly coated with thickness controlled, smooth and homogeneous silica shells *via* the standard Stöber method by varying the amount of tetraethoxysilane (TEOS). Compared with methods reported in the literature for the coating of such particles, this method can not only be used to successfully coat citrated-stabilized Au or Ag NPs, but can also be extended to encapsulate oleylamine (OA)-stabilized Au NPs and cetyltrimethylammonium bromide (CTAB)-stabilized Au nanorods (NRs) by using MUA to displace the original ligand on the surface of the NPs. Additionally, the obtained metal@SiO_2 core–shell NPs have been successfully applied as plasmonic nanoantennas for fluorescence enhancement in metal@SiO_2@fluorophore NPs.

1 Introduction

Noble metal NPs have found significant potential applications in the fields of catalysis,[1] optics,[2] and biosensing.[3–5] A prerequisite for these applications is suitable surface functionalization which determines their interaction with the environment, since it is directly related to the colloidal stability of the NPs, and controls the assembly or targeting of the NPs. In this respect, silica coating is one of the most popular methods,[6] mainly due to the anomalously high stability of silica, especially in aqueous media. This method is superior in its easy regulation of the coating process, chemical inertness, controlled porosity, good processability, and optical transparency. On top of that, silica shells are easily labeled with various functional groups.[7] In particular, metal nanostructures exhibit remarkable optical properties due to excitation of their surface plasmons by incident light, which results in a significant enhancement of the electromagnetic field at the NP surface. This leads to various optical enhancement effects, such as enhanced luminescence.[8,9] Previous investigations of plasmon-enhanced fluorescence were carried out on metal NP films.[10] Core–shell nanostructures consisting of metallic NPs coated with a shell of silica doped with a suitable fluorophore that display enhanced luminescence were reported recently.[8,9] These core–shell NPs provide several advantages. For example, the metal core improves excitation efficiency and enhances the emission rates, ensuring the reduced self-quenching of the fluorophores. The silica shell can provide a versatile surface for functionalization. Importantly, the silica shell separates the fluorophore from the metal core in order to avoid quenching by metal core.[8,9]

The Stöber method has become a popular approach to coat noble metal NPs with silica shells.[6,11] However, applying the Stöber method to directly coat silica shells on metal NPs has long been hindered because noble metal NPs are not stable in alcoholic solutions and have low chemical affinity for silica.[11] Therefore, most of the reported silica coating routes are based on the surface modification of the metal NPs. Mulvaney *et al.* and Matijevic *et al.* first reported that noble metals, such as citrate-stabilized Au and Ag, could be coated with a silica shell using a silane coupling agent to induce the formation of a thin

[a]*State Key Laboratory of Luminescence and Applications, Changchun Institute of Optics, Fine Mechanics and Physics, Chinese Academy of Sciences, Changchun 130033, P. R. China. E-mail: xgkong14@ciomp.ac.cn; Tel: +86 431-86176313*

[b]*Graduate University of the Chinese Academy of Sciences, Beijing, 100049, P. R. China*

[c]*Van't Hoff Institute for Molecular Sciences, University of Amsterdam, Science Park, P. O. Box 94157, 1090 GD Amsterdam, The Netherlands. E-mail: h.zhang@uva.nl; Fax: +31 20 525 5604; Tel: +31 20 525 6976*

† Electronic supplementary information (ESI) available: The influence of MUA-modified Au or Ag NPs and silica encapsulation on the UV-vis absorption spectra, the effect of different '*n*' for SH–$(CH_2)_n$–COOH compounds on the encapsulation of Au NPs with silica, FE-SEM images of silica-coated Au NRs with different silica shell thicknesses. See DOI: 10.1039/c3tc31171f

silica shell by sodium silicate condensation prior to solvent exchange and subsequent growth by means of the Stöber method.[12,13] Graf *et al.* coated noble metal NPs with silica by adsorbing poly(vinyl pyrrolidone) onto the NP surface as a primer.[14] Surfactants, polyelectrolytes, enzymes, and gelatin were also used for the construction of metal@silica core–shell NPs.[15–18] The synthesis of metal@silica core–shell NPs has also been reported without the use of primers.[19,20] However, these methods were only valid for coating relatively large colloidal particles (>50 nm) of noble metals, because smaller particles were unstable and tended to aggregate during the Stöber process.[21] In addition to hydrophilic metal nanoparticles, hydrophobic metal nanoparticles have also been interfaced by ligand-exchange followed by silica growth.[22] For all the above methods, the role of the surface priming is not only to increase the affinity of the metallic surface towards silica, but also to provide the colloids with sufficient stability to be transferred into ethanol or isopropanol so that the classical Stöber method can be used. Today, it is desirable to develop a more versatile, reproducible coating strategy independent of the phase and morphology of the noble metal NPs.

Due to the strong metal–S bond reaction, thiols can replace the standard capping agents from the surfaces of metal NPs.[23] The adsorption of thiols on the surface of noble metals, such as Au or Ag, has been intensely studied and widely used.[24–28] Au and Ag NPs synthesized with oleylamine (OA) in toluene could be transferred to an aqueous phase when OA was replaced by a thiol compound.[29] The same principles were also applied to Au rods, where the replacement of the CTAB double layer with thiol-containing PEG was reported.[30,31] So using thiol compounds as a primer has the potential to allow the development of a more versatile, reproducible silica coating strategy, independent of the sizes, shapes and phases of the metal NPs, if the other end of the thiol compound has an affinity for silica. 3-Mercaptopropyl triethoxysilane was used as a primer to successfully coat Au NPs with a silica shell.[32] However, a subsequent article has demonstrated the method was not general.[16] Liz-Marzán *et al.* also used a thiol-modified PEG as primer to replace the standard capping agents of Au NPs with different sizes and shapes.[30] However, the thiol-modified PEG was not typical of thiol compounds. Firstly, obtaining the thiol-modified PEG required a complicated synthesis procedure. Secondly, the thiol-modified PEG was very expensive. Thirdly, in the core–shell NPs a thick and poorly defined interface layer was present because of the bigger molecular weight of PEG. Thiol compounds with the structure HS–$(CH_2)_n$–COOH are much more common and cheaper. Importantly, a recent study demonstrated that the –COOH groups show chemical affinity for silica,[33] which indicates that HS–$(CH_2)_n$–COOH may be a good primer for silica coating of noble metal NPs.

In this work, MUA was proposed and validated as a bifunctional molecule to successfully encapsulate noble metal NPs in different phases and/or different morphologies and/or with different surfactants. Here, MUA was bound to the noble metal surface *via* a metal–S bond, and the –COOH group was used as the active group to facilitate the hydrolysis/condensation of tetraethoxysilane (TEOS). It was demonstrated that MUA could be used to coat a thickness-adjustable, homogeneous silica shell not only on citrate-stabilized Au and Ag NPs, but also on CTAB-stabilized Au nanorods (NRs) and OA-stabilized Au NPs, based on the fact that the weakly absorbed OA or CTAB on the NPs can be readily displaced by thiols from MUA. The experimental results from varying the '*n*' for SH–$(CH_2)_n$–COOH ($n = 2$, 10 or 15) of the primer demonstrated that the affinity of carboxyl to silica was related to the value of '*n*'. To the best of our knowledge, this is the first report of successfully using MUA as the linker molecule to coat noble NPs with silica. We have applied the metal NPs as plasmonic nanoantennas to enhance the fluorescence of fluorescein isothiocyanate (FITC) by synthesizing metal@SiO_2@fluorophore NPs, proving that the present NPs acted as excellent plasmonic nanoantennas.

2 Materials and methods

2.1 Materials

3-Mercaptopropionic acid (MPA), 11-mercaptoundecanoic acid (MUA), 16-mercaptohexadecanoic acid (MHA), $HAuCl_4$ (99.99%) and 3-aminopropyl-trimethoxysilane (APS) were purchased from Aldrich. Tetraethyl orthosilicate (TEOS, 98%) and FITC (90%) were purchased from Fluka. Sodium citrate (A.R.) was obtained from Beijing Chemical Plant. Fluorescamine was obtained from Shanghai Aladdin Industrial Corporation. Hexadecyltrimethylammonium bromide (CTAB, ~99%) and L-ascorbic acid (≥99.5%) were purchased from Sigma. Silver nitrate ($AgNO_3$, ≥99%) was purchased from Fluka. All the chemicals were used as received without further purification. Deionized water was purified using a Milli-Q water purification system, and the resistivity was 18.2 MΩ cm.

2.2 Synthesis

The general procedure to coat noble metal NPs with silica consists of two steps: synthesis of thiol-coated NPs and growth of the silica shell after transfer of the NPs to ethanol. An outline of the synthesis is shown in Fig. 1.

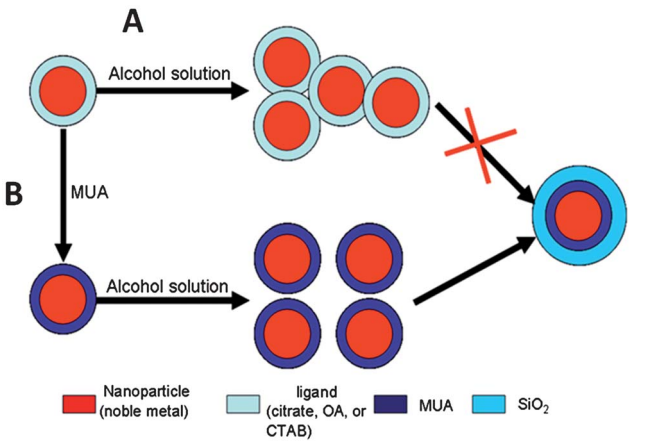

Fig. 1 Diagram of the general procedure for coating silica on NPs. (A) The original NPs cannot be dispersed in alcoholic solution. (B) MUA is exchanged with the ligand on the NPs' surface, followed by growth of the silica shell because of the chemical affinity of –COOH for silica.

Synthesis of the colloids

Gold NPs with a diameter of 15 nm. Au NPs were prepared according to the standard sodium citrate reduction method. Typically, 50 mL deionized water and 1 mL $HAuCl_4$ (1%) aqueous solution were mixed in a three-neck flask and heated to 100 °C. Subsequently, 0.8 mL of 5% sodium citrate solution was quickly added to the flask. The color of the solution rapidly changed from a yellow tint to deep red. After one hour, the Au NPs were cooled down to room temperature and kept ready for modification with MUA.

Gold NPs with a diameter of 40 nm. In order to grow larger Au NPs we used a seeded growth method.[34] Specifically, 30 mL of the solution of 15 nm Au seeds was mixed with 20 mL of H_2O and 2.4 mL of 5% sodium citrate in a 100 mL flask and heated to 70 °C. Then 3 mL 1% $HAuCl_4$ solution was slowly added to the mixture. 60 min later, the solution was cooled down to room temperature.

Synthesis of oleylamine (OA)-coated Au NPs in oil phase. OA-coated Au NPs were prepared following the reported procedure.[29] 50 mg (0.15 mmol) of $HAuCl_4$ in 1.0 g of oleylamine and 1.0 mL of toluene were added to a boiling solution of 1.7 g of oleylamine in 49 mL of toluene. Heating was stopped after 2 h, followed by cooling down to room temperature.

Synthesis of Au nanorods (NRs). The synthesis of Au NRs was a seed-mediated growth procedure,[35] in which Au salt was reduced initially with a strong reducing agent in water at room temperature. In brief, the Au seed particles were prepared by reduction of $HAuCl_4$ (0.25 mM) in CTAB solution with ice-cold sodium borohydride as the reducing reagent. Subsequent reduction of more metal salt with a weak reducing agent in the presence of structure-directing additives, lead to the controlled formation of gold nanorods. Briefly, a 25 mL growth solution was prepared by reduction of 0.5 mM $HAuCl_4$ in a solution containing CTAB, 0.05 mM silver nitrate and 176 μL of ascorbic acid. The color of the solution rapidly changed from golden to colorless after the introduction of ascorbic acid. 36 μL of the seed solution was then added to the growth solution, and the color of the solution slowly changed from colorless to deep purple. Ultimately, bilayer CTAB-coated gold nanorods were obtained after several hours' stirring.

Synthesis of Ag NPs. The synthesis of Ag NPs was a stepwise reduction method. We used $NaBH_4$ to control the nucleation stage of the reaction, and sodium citrate as a reducing agent in the growth process. The particle size decreased with the

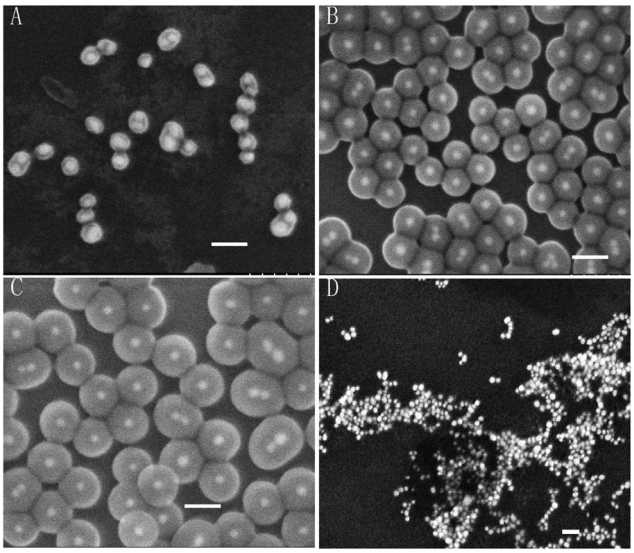

Fig. 3 FE-SEM of silica-coated Au NPs 15 nm in diameter produced by varying the amount of TEOS (A)–(C). The shell thicknesses were 7 nm (A), 15 nm (B) and 22 nm (C). (D) FE-SEM of silica-coated Au NPs with Tween 20 and MUA purified only once by centrifuge. The scale bar is 60 nm.

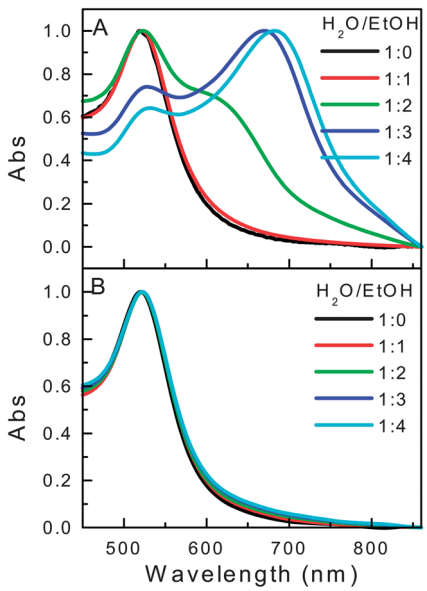

Fig. 2 Normalized optical absorption spectra of Au NPs (15 nm in diameter) with different ratios of water to ethanol: (A) citrate-stabilized Au NPs; (B) MUA-modified Au NPs.

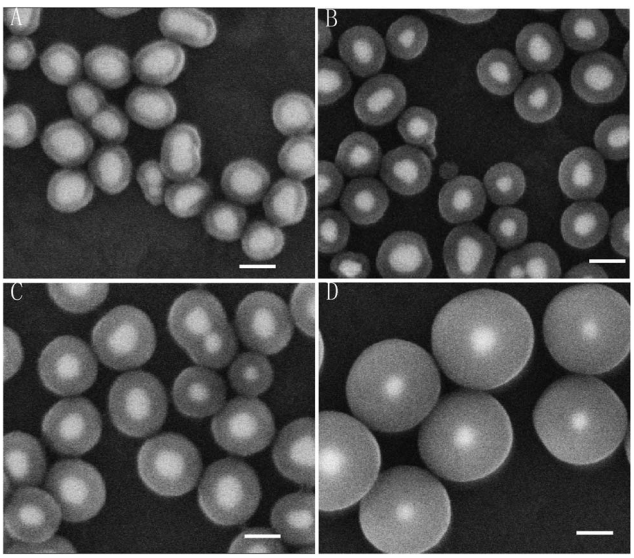

Fig. 4 FE-SEM of silica-coated Au NPs (the diameter of the Au NPs is 40 nm) produced by altering the amount of TEOS added. The shell thicknesses are 15 nm (A), 20 nm (B), 30 nm (C) and 60 nm (D). The scale bar is 60 nm.

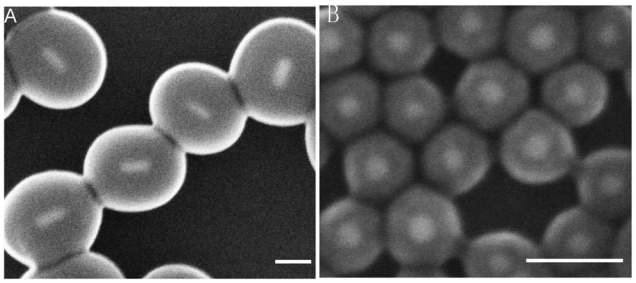

Fig. 5 FE-SEM of silica-coated Au NRs (A) and OA-modified Au NPs (B). The scale bar is 60 nm.

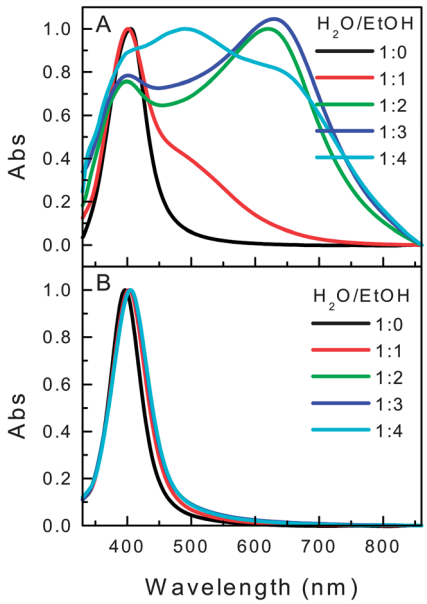

Fig. 6 Normalized optical absorption spectra of Ag NPs with different ratios of water to ethanol: (A) citrate-stabilized Ag NPs; (B) MUA-modified Ag NPs.

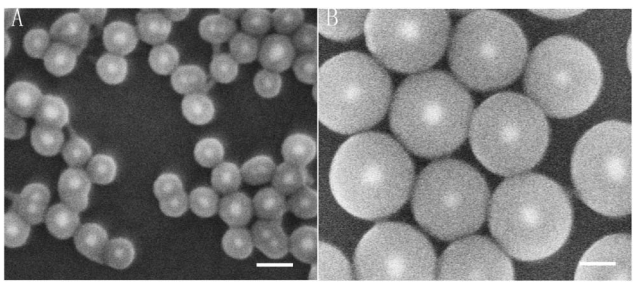

Fig. 7 FE-SEM of silica-coated 20 nm Ag NPs produced by varying the amount of TEOS. The shell thicknesses are 20 nm (A) and 60 nm (B). The scale bar is 60 nm.

increase of $NaBH_4$ concentration due to the increasing concentration of silver nuclei reduced by $NaBH_4$. Typically, in a 50 mL deionized water solution, the concentrations of $AgNO_3$, sodium citrate and $NaBH_4$ were 1×10^{-3} M, 7×10^{-3} M and 1×10^{-6} M, respectively. The above solution was stirred rapidly at 4 °C for 1 min. Then, the solution was heated to 100 °C. The heating was stopped after half an hour and cooled down to room temperature, and the NPs were kept ready for modification with MUA.

Synthesis of thiol-coated Au NPs. The synthesis of thiol compounds-coated NPs was a two step method.[36] Importantly, in this method, before performing the chemisorption of MUA on the Au NPs' surface, Tween 20 was firstly physisorbed onto the citrate-stabilized Au NPs. Direct surface modification using thiol chemistry results in particle aggregation, which can be avoided by forming a physisorbed monolayer of the nonionic surfactant Tween 20 on the surface prior to the chemisorption of alkanethiols. The adsorbed layer of Tween 20 prevents the NPs from aggregating in the subsequent reaction. MUA penetrated through the Tween 20 layer and displaced the underlying anionic citrate and chloride. When the new protection layer had been established, Tween 20 was removed and the NPs remained stable.[36] 40 mL of Au NPs and 8 mL of Tween 20 (2% v/v) were gently mixed and allowed to stand for a minimum of 20 min to allow the physisorption of Tween 20 onto the Au NPs. The thiol solution was then added and the final mixture (final concentrations: [Au NPs] = 0.27 nM, [alkanethiols] = 0.54 μM) was left to stand for up to 12 h. Excess thiols and Tween 20 were removed from the surface-modified colloids by centrifugation for 15 min at 11 500 rpm, followed by decantation of the supernatants and resuspension in water. All solutions containing colloids were stored in glass tubes in the dark to prevent light-induced flocculation of the colloids and oxidation of the alkanethiolates.

Synthesis of thiol-coated Ag NPs. The synthesis of MUA-coated Ag NPs was as same as for the Au NPs. 40 mL of Ag NPs and 16 mL of Tween 20 (2% v/v) were gently mixed and allowed to stand for a minimum of 20 min to allow the physisorption of Tween 20 onto the Ag NPs. The MUA in ethanol solution was then added and the final mixture (final concentrations: [Ag NPs] = 0.27 nM, [alkanethiols] = 1.08 μM) was allowed to stand for up to 12 h. Excess thiols and Tween 20 were removed from the surface-modified colloids by centrifugation for 15 min at 11 500 rpm, followed by decantation of the supernatants and resuspension in water. All solutions containing colloids were stored in glass tubes in the dark to prevent light-induced flocculation of the colloids and oxidation of the alkanethiolates.

Synthesis of thiol-coated Au NPs (OA-coated Au NPs). MUA-coated Au NPs were obtained by adding 4 mg of Au NPs dissolved in 2.0 mL of toluene to a boiling solution of 5–10 mole equivalents of the ligand (MUA) in toluene. The reaction was protected by an Ar environment. Excess MUA was removed from the surface-modified colloids by centrifugation for 15 min at 11 500 rpm, followed by decantation of the supernatants and resuspension in water.

Synthesis of thiol-coated Au NRs (CTAB-coated Au NRs). The solubility of the CTAB-stabilized Au NRs was much lower than that of the citrate-stabilized Au NPs, and they started to aggregate when the ratio of ethanol to water was greater than 0.25. Due to the relatively strong binding of the surfactant to the CTAB-stabilized Au NRs compared to citrate-stabilized ones, the coupling reaction of MUA to the Au NR surface was different from the approach for the citrate-stabilized Au NPs. MUA dissolved in ethanol was added directly to the aqueous solution of

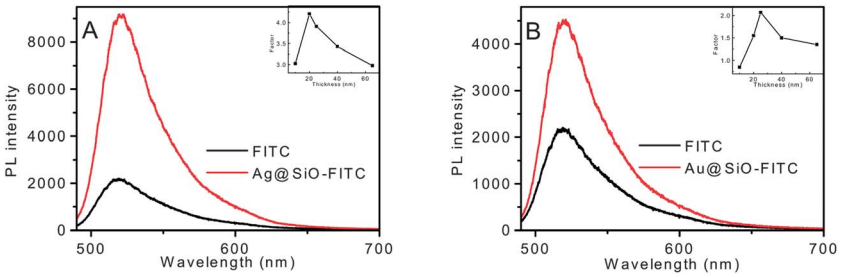

Fig. 8 Emission spectra of (A) Ag@SiO_2–FITC with a FITC–metal distance of 20 nm, and (B) Au@SiO_2–FITC with a FITC–metal distance of 25 nm. Distance dependent enhancement factors of the FITC by Ag and Au NPs are shown in the insets.

Au NRs, and the ratio of ethanol : water was set at 1 : 9. After 12 h, the solution was centrifuged once for 15 min at 8000 rpm.

Encapsulation of the thiol-coated noble metal nanoparticles with silica shells. The growth of silica shells on colloidal particles by the Stöber method is usually performed in an ethanol–ammonia mixture. If the total surface area of the seed particles per volume is large enough compared to the added amount of TEOS, the formation of new silica particles can be completely suppressed and therefore the thickness of the silica shell can be precisely controlled by the amount of TEOS added.

The as-prepared thiol-coated nanoparticle solution (20 mL) was mixed with isopropanol (80 mL) in a 150 mL glass conical tube. Under vigorous stirring, ammonia (1.92 mL, 30 wt%) was added to the mixed solution, followed by the addition of TEOS in isopropanol (0.6 mL, 10 mM) four times within 6 h (at time intervals of 2 h). After stirring for 18 h, the reaction mixture was then centrifuged at 8000 rpm for 15 min and the colloid–SiO_2 NP precipitate was redispersed in ethanol for further washing. After washing three times, colloid–SiO_2 NPs were obtained and redispersed in deionized water or ethanol (5 mL) for characterization and further functionalization. The shell thickness of the colloid–SiO_2 particles could be easily controlled by the amount of TEOS added.

Of course, controlling the thickness of silica could be performed by changing the reaction time. However, this method is not reproducible. So in our work we controlled the thickness of silica shell by changing the amount of TEOS. For different kind of NPs, the amount of TEOS added depended on the surface area of the NPs.

Synthesis of metal@SiO_2@FITC NPs. Approximately 10 mg of NPs were dispersed in 1 mL of deionized water with sonication and mixed with 20 μL of glacial acetic acid. 10 μL of APS was added with sonication, and the suspension was stirred for 4 h. The NPs were washed three times using ethanol and then dispersed in ethanol.

4 mg of FITC was first dissolved in 3 mL of ethanol, followed by the addition of APS-modified metal@SiO_2. The reactants were allowed to react in the dark for 24 h under stirring. The reaction was purified by centrifugation at 11 500 rpm for 15 min.

2.3 Characterization

The size and morphology of the colloids were characterized by field emission scanning electron microscopy (FE-SEM, Hitachi, S-4800). Ultraviolet-visible (UV-vis) absorption spectra were measured at room temperature using a UV-3101 spectrophotometer. The fluorescence spectra were measured at room temperature by a Jobin-Yvon LabRam Raman spectrometer system equipped with 600 grooves mm^{-1} holographic gratings and a Peltier air-cooled CCD detector.

3 Results and discussion

Fig. 1 is a schematic illustration of the synthesis of the nanoparticle–silica core–shell nanostructures using MUA as a linker. Without MUA, the Au NPs start to aggregate immediately when the citrate-stabilized Au NPs are transferred from water solution to alcohol solution, and finally precipitate at the bottom, which makes them not suitable for coating. With MUA, the citrate-stabilized Au NPs will react with MUA, as MUA can strongly bind to the Au NP surface *via* Au–S bonds by replacing the Au–citrate. Because MUA is soluble in alcoholic solutions, the MUA-modified metal NPs will be stable in alcoholic solutions. In the meantime, the carboxyl-terminated surfaces are active for the nucleation and deposition of silica.[33] Therefore, the deposition of silica shells on the surface of the MUA-functionalized Au NPs can be easily performed in a water and alcohol mixed solution *via* the Stöber method.

It is important to stress that this procedure is reproducible and versatile, and can be used for silica coating on Ag NPs, CTAB-stabilized Au NRs, OA-stabilized Au NPs, *etc.*, in either water or oil phase. The following are several examples.

Coating of Au colloids

As mentioned previously, directly applying the Stöber method to coat citrate-stabilized Au NPs is valid only for large colloidal particles (>50 nm) of noble metals, because smaller particles are unstable and tend to aggregate during the Stöber process.[19–21] Therefore, a detailed discussion of the method for using MUA as a linker molecule to coat noble metals is presented for the coating of small Au particles.

Following the Stöber method, the coating of silica on the Au NPs can only be performed in an ethanol–water mixture, and the ratio of ethanol to water must be greater than 3, which requires that the Au NPs must be stable in an ethanol–water mixture. A prevalent and efficient method to investigate the state of NPs in solution is the measurement of the UV-visible

extinction spectrum.[36] Relevant UV-vis spectra were measured to monitor the stability of the synthesized citrate-stabilized Au NPs in ethanol–water mixture solutions, as shown in Fig. 2A. The absorption spectra of the freshly prepared Au NPs solution presented a strong extinction band with a maximum at 520 nm, characteristic of the collective excitation of the free conduction band electrons of the NPs, known as the surface plasmon resonance. With the increase of the ratio of ethanol to water from 0 to 4, a significant change in the absorption spectra was observed. A new broad band appeared on the red side of the spectra from 600 to 700 nm, moving gradually towards longer wavelength. At the same time, the surface plasmon resonance band at 520 nm tailed off and showed a red shift. This was a consequence of small aggregate clusters of the nanoparticles, as predicted by Mie theory.[37] The morphology of the aggregates was observed by FE-SEM, where the formation of linear arrays rather than compact clusters of NPs was confirmed. Clearly, the new long wavelength band (600–700 nm) was associated with the longitudinal mode of the electronic plasma oscillation along the long axis of the linear colloidal aggregates. The transverse mode retained a location similar to the sphere resonance mode. Liao *et al.* also observed the linear aggregation phenomenon of Au NPs in an ethanol–water mixture solution, which was ascribed to the addition of ethanol which destroyed the surface charge of Au NPs and resulted in the aggregation of the Au NPs.[38] The above results demonstrated that the Stöber method was not applicable for the direct silica coating of citrate-stabilized Au NPs.

Therefore, prior to silica coating, a new interface has to be designed by using a bifunctional molecule as a primer, which not only facilitates the hydrolysis/condensation of tetraethyl orthosilicate (TEOS), but also provides the colloids with sufficient stability to be transferred into ethanol.

It is well known that thiols can be linked on the surface of Au NPs *via* the Au–S bond, and the –COOH group shows chemical affinity for silica.[33] The following work was to research whether SH–$(CH_2)_{10}$–COOH (MUA) could be used as a new primer. Here we characterized the influence of MUA-modification on the Au NPs from the absorption spectra, as shown in Fig. S1.† The spectra revealed an absorption maximum of MUA-modified Au NPs, $\lambda_{max} = 523$ nm, which meant that ligand exchange caused the absorption maximum to shift towards the red by 3 nm. This was in agreement with previously reported SPR shifts resulting from local dielectric constant changes near the metal core.[39] Additionally, the spectral shift was not accompanied by broadening of the spectrum, indicating a lack of NP aggregation.[36]

The stability of the MUA-modified Au NPs in ethanol–water mixed solution was confirmed by UV-vis absorption spectra, as shown in Fig. 2B. Little difference was observed in the UV-vis absorption spectra when the ratio of ethanol to water varied from 0 to 4, except for a slight red shift. The red shift is correlated directly with the change in the dielectric constant of the medium around the NPs. The lack of spectral broadening supported the conclusion that the as-synthesized NPs remained monodisperse.

Finally, we turned to follow the Stöber method to produce a silica shell, using TEOS, on the MUA-modified Au NPs. This method involved the base-catalyzed hydrolysis of TEOS to generate silica sols, followed by nucleation and condensation of these sols on the surfaces of the Au NPs. In our experiment, ammonia was added as a catalyst to speed up the hydrolysis of the TEOS precursor. In fact, if the amount of TEOS could be precisely added according to the total surface area of the seed particles by volume, the formation of the isolated silica particles would be completely suppressed, *i.e.* the thickness of the silica shell on the seed can be accurately controlled in this way. Here, we controlled the thickness of silica shell simply by repeatedly adding TEOS into the reacting solution at time intervals of 2 h. Fig. 3A–C show the FE-SEM images of Au NPs coated with different thicknesses of silica shells by varying the TEOS amounts. For all three samples, no secondary nucleation of small silica colloids was observed, confirming the sufficiently high total particle surface per volume. It is worth noting that the silica shell was homogeneous on each individual Au particle, regardless of its original morphology. As a result, the shape of each Au NP was essentially retained during the silica coating, especially when the shell was relatively thin (Fig. 3A). In this case, the polydispersity of the original NPs was also maintained. As the thickness of silica coating increased, the core–shell NPs became more monodisperse because of a reduction in the relative size distribution. In the following work, we researched the influence of Tween 20 in solution on the silica encapsulation. Fig. 3D shows the FE-SEM image of silica-coated Au NPs when the Tween 20 and MUA were only purified once by centrifugation. This image confirmed that the Au NPs only aggregated when they were not coated with silica. Moreover, isolated silica NPs were not formed, demonstrating that the superfluous Tween 20 in the solution interfered with the nucleation of silica. Therefore the MUA-modified Au NP solution had to be purified before encapsulation with the silica shell. The generation of Au–silica core–shell NPs with a homogenous silica shell structure indicated that the core surface presented strong chemical affinity between –COOH and silica.

At the same time, the influence of the number of $-CH_2-$ groups in HS–$(CH_2)_n$–COOH on the silica encapsulation was also studied by using the other ligands, such as MPA (SH–$(CH_2)_2$–COOH) or MHA (SH–$(CH_2)_{15}$–COOH) (see Fig. S2†). The results showed that the affinity of the carboxyl group for silica of the SH–$(CH_2)_n$–COOH ($n = 2$, 10 or 15) ligand is also related to the value of 'n'.

We have also studied the influence of the silica shell on the optical properties of Au NPs in ethanol (see Fig. S3†). Initially, with increasing shell thickness, a red shift was observed in the absorption maximum due to the increase in the local refractive index around the NPs. When the silica shell was sufficiently thick, the scattering became non-negligible, resulting in an enhancement at the longer wavelength side. However, there was no significant change in the peak position, and the colors of the dispersions before and after coating remained essentially the same. Further increasing the silica thickness did not alter the absorption spectrum any more. This observation was consistent with the observation of Mulvaney *et al.*[12]

In the above experiments, the diameter of the Au NP was 15 nm. To further demonstrate the feasibility and universality of this method, a bigger size Au NPs, 40 nm in diameter, were also

coated. The obtained Au NPs became quite unstable when transferred into alcoholic solution for silica coating. Within seconds to minutes, the Au NPs started to aggregate and eventually formed a dark blue solution. The behavior was the same as that of the 15 nm Au NPs. Following the same procedure of MUA modification for the 15 nm Au NPs before silica coating, and varying the thickness of silica shell by controlling the addition amount of TEOS, homogeneous silica coated NPs were readily obtained. Fig. 4 shows the Au–SiO_2 NPs with a 40 nm core and different shell thicknesses. For all four samples, no secondary nucleation of small silica colloids was observed, resulting from the sufficiently high total particle surface per volume. Due to the bigger size, the FE-SEM images can clearly show the homogeneous shell of each individual Au particle, regardless of its original morphology (Fig. 4A). In this case, the polydispersity of the original NPs was also maintained.

A similar method was used to coat Au NRs. Au NRs are elongated NPs with distinctive optical properties that depend on their shape.[40] In particular, they possess two principal plasmon absorption bands: one is the transverse plasmon band, corresponding to light absorption and scattering along the short axis of the particle, and the other is the longitudinal plasmon band, that along the long axis of the particle. The former is located in the visible region of the electromagnetic spectrum at *ca.* 520 nm, while the latter can be tuned by the aspect ratio of the Au NRs from the visible to the near-IR region. Additionally, the elongated NPs have an inherently higher sensitivity to the local dielectric environment as compared to similar sized spherical NPs.[41] The above properties make them more interesting for a wide variety of applications compared to Au NPs. The surface ligands of Au NRs are cetyltrimethylammonium bromide (CTAB), which prevent Au NRs from further modification and forbid their application. Moreover, the stability of Au NRs is dependent on the presence of CTAB molecules in a narrow concentration range close to its critical micelle concentration.[16] Silica coating of Au NRs is an attractive alternative for their manipulation and for providing enhanced colloidal stability. Several procedures have been developed for the silica coating of Au NRs, such as the polyelectrolyte layer-by-layer (LBL) technique.[16] There are a couple of methods for silica coating of citrate-stabilized gold NPs using surface primers, such as aminopropyltrimethoxysilane (APS) and poly(vinylpyrrolidone) (PVP).[12,14] These methods, however, have been found to fail for the coating of Au NRs.[16] The polyelectrolyte multilayer and mPEG remain in the core–shell particle as a thick and poorly defined interface layer.[16,30]

The solubility of the CTAB-stabilized Au NRs was much lower than that of citrate-stabilized Au NPs, and they started to aggregate when the ratio of ethanol to water was greater than 0.25. Due to the relatively strong binding of the surfactant to the CTAB-stabilized Au NRs compared to the citrate-stabilized ones, the coupling reaction of MUA on the Au NR surface was different from the approach for citrate-stabilized Au NPs. Using the above method for MUA-modified citrate-stabilized Au NPs, 4 MUA molecules per nm^2 proved that MUA-modified Au NRs could not be coated with silica. In a systematic study, it was found that complete homogeneous silica shells could be obtained when a significant excess of MUA molecules was used, corresponding to 60 molecules per nm^2. The FE-SEM image in Fig. 5A shows the effectiveness of this method for the deposition of silica shells. A uniform thickness of silica shells appeared around all facets of the NRs. Similar to the case of NPs, the thickness of the silica shell could easily be adjusted by controlling the amount of TEOS. Fig. S4† shows another two Au–SiO_2 core–shell nanostructures with different shell thicknesses. As the amount of TEOS increased, the silica shell thickness increased from 30 nm to 60 nm. The effect of these silica shells on the optical response of these particles is displayed in Fig. S5.† Whereas the longitudinal surface plasmon band is found to red shift by as much as 13 nm because of the local refractive index increase, the transverse plasmon band remains basically unaltered at 518 nm. This result agrees with previous reports and with the higher sensitivity of Au NRs as compared to spheres.[30]

So far we have demonstrated that the MUA-assisted silica coating method was effective for water-phase Au NPs. In the following work, the procedure was also demonstrated to coat OA-stabilized Au NPs synthesized in an oil phase. For the citrate reduction method, the difficulty in controlling the nucleation and growth steps occurs at the intermediate stages of particle formation, resulting in a broad particle size distribution, whereas the Au NPs synthesized in the oil phase possess lower polydispersity. However, in order to extend the application of Au NPs synthesized in oil phase to, *e.g.* biological and medical fields, the NPs need to be hydrophilic, and silica coating is a popular approach. Similar to the procedure for water-phase NPs, the Au NPs synthesized in oil phase can also be coated with silica by using MUA as a primer. A coating of 60 MUA molecules per nm^2 was shown to grow silica on the Au NP surface. The experimental procedure for the encapsulation by silica was the same as for citrate-stabilized Au NPs. The FE-SEM images in Fig. 5B show the effectiveness of this method for coating with a silica shell.

Other noble metal particles – Ag NPs

Silver NPs, as an important member of the noble metal nanomaterials, have also been studied in depth because of their promising applications in various fields such as biological catalysis, detection, sterilization, electronics and optics.[42] It is necessary to develop or utilize robust surface chemistry that will not only protect the silver NPs from aggregation but also render them amenable to further application. It is desirable to coat the silver NPs with a shell of pure silica to permanently preserve their optical properties for effective functionalization.

The absorption spectra of the freshly prepared Ag NPs solution presented a strong absorption band with a maximum at 405 nm, and the full width at half-maximum (FWHM) was only 67 nm, which was much smaller than that of those prepared by the citrate reduction method (120 nm FWHM).[42] Similar stability problems to those of the Au NPs were found in ethanol–water mixed solution from the UV-vis absorption spectra. On increasing the ratio of ethanol to water from 0 to 4, a significant change in the absorption spectrum was observed, as shown in Fig. 6A. As the ratio of ethanol to water increased, a

new broad band gradually appeared on the red side of the spectra, moving towards longer wavelength from 500 to 700 nm, accompanying the decrease and blue shift of the surface plasmon resonance band at around 405 nm. Similarly, the above explanation for the aggregation phenomenon of Au NPs in an ethanol–water mixture could also apply to the Ag NPs.

MUA was used as a linking molecule to modify the surface of Ag NPs by a similar procedure to that for Au NPs. The optical properties of Ag NPs are shown in Fig. S6.† The absorption maximum was located at around 410 nm. After ligand exchange, the absorption maximum shifted to the red by 5 nm, which was a greater shift than that of Au NPs (3 nm), indicating that the Ag NPs were more easily influenced by the environment. The lack of aggregation was also supported by the negligible spectral broadening.[36]

Using the same procedure as that for the Au NPs, MUA-stabilized Ag NPs in ethanol–water mixed solution with were obtained. Fig. 6B shows the UV-vis absorption spectra of MUA-modified Ag NPs in ethanol–water solutions with different ratios. Little difference was observed from the UV-vis spectra as the ratio of ethanol to water was increased from 0 to 4, except for a slight red shift which was correlated with the change of the dielectric constant of the medium around the NPs.[39] The red shift (9 nm) of Ag NPs was bigger than that of the Au NPs (2 nm).

The above experiments proved that the MUA-stabilized Ag NPs could be transferred into ethanol solution. In the past, many studies of the encapsulation of Ag NPs with silica have shown that Ag NPs are etched by ammonia. To solve this problem, dimethylamine was used as an alternative to ammonia to catalyze the growth of silica shells on the Ag NPs.[43,44] However, similar to the Au NPs using ammonia as a catalyst, a silica shell was readily formed on the MUA-modified Ag NPs. The resulting monodisperse Ag NPs with homogeneous shells are shown in Fig. 7. The results indicate that the MUA on the Ag NP surface can hinder the etching effect of ammonia.

The influence of the silica layer on the optical properties of Ag NPs with a diameter of 20 nm is shown in Fig. S7.† The thickness of the silica shells varied in the range of 20 to 60 nm. Compared to the peak position of the Ag NPs (see Fig. 6B), the absorption maximum shifted to the red from 410 nm to 420 nm, resulting from the increase in local refractive index around the particles.[39] When the silica shell thickness changed from 20 nm to 60 nm, scattering became significant. All these effects are accounted for by Mie's theory for core–shell particles.

As discussed above, realization of the coating of NPs with silica shells by the Stöber method must satisfy two conditions: the colloids should be stable in a water–ethanol mixed solution, and the surfaces of colloids must have significant chemical affinity with silica. The main role of the MUA modification is to enhance the colloidal stability so that the NPs can be dispersed in an ethanol–ammonia mixture without aggregation and silica coating can be carried out through the Stöber method. Additionally, MUA can serve as a primer to facilitate the condensation of silica on the metal surface.

So far, we have described a general strategy to coat spherical and rod-shaped Au NPs with silica shells. Moreover, this method can also coat OA-stabilized Au NPs dispersed in an oil phase. We suggest that this method might be readily extended to any MUA-coated colloid. An another advantage of this method over reported ones is that it readily provides fine control over the thickness of the silica shells by simply varying the amount of TEOS. This is clearly demonstrated by the FE-SEM images in Fig. 3 and 4 for multistep silica coating of Au NPs.

Synthesis of metal@SiO_2@FITC NPs

In the following, we demonstrate that these metal@SiO_2 NPs are suitable candidates as plasmonic nanoantennas to enhance the fluorescence of fluorophores. In this kind of composite NPs, Au or Ag cores provide the high electromagnetic field necessary to enhance the fluorescence signal of a given fluorophore. The silica shell additionally provides the colloid with high colloidal stability as well as an ideal surface for functionalization. More importantly, the silica shell can separate the fluorophore from the metal core to avoid quenching by the metal core and tune the enhancement effect.[8,9] A demonstration of this capability was carried out with 15 nm Au spheres and 20 nm Ag spheres. The enhancement factor was measured by titration experiment. Firstly, FITC was dispersed in 5 mL of ethanol solution with a concentration of 50 nM. Then the APS-modified metal@SiO_2 NPs were added to the FITC solution. Finally, when the measured fluorescence intensity was almost unchanged, the obtained intensity was taken to be the biggest enhancement. The emission spectra of Ag@SiO_2–FITC and Au@SiO_2–FITC, as well as the comparison with their FITC reference control are presented in Fig. 8. All fluorescence spectra were measured with an excitation wavelength of 488 nm from an Ar^+ laser. The fluorescence enhancement factor was defined as the ratio of the fluorescence intensity of Ag@SiO_2–FITC and Au@SiO_2–FITC to the fluorescence intensity of the control. Fig. 8 presents the best fit enhancement fluorescence for different metal cores. As shown in Fig. 8, the fitted enhancement factors for Ag@SiO_2–FITC and Au@SiO_2–FITC are 4.21 and 2.07, respectively. The fitted silica shell thicknesses for Ag@SiO_2–FITC and Au@SiO_2–FITC are 20 nm and 25 nm, respectively.

4 Conclusions

We have developed a reproducible and versatile approach to effectively coat a thickness-adjustable and homogeneous silica shell on noble metal NPs of different morphologies and in different phases, including citrate-stabilized Au and Ag NPs, CTAB-stabilized Au NRs and OA-stabilized Au NPs. The chemical process of silica deposition was facilitated by a monolayer of MUA on the surface of the noble metal NPs. The MUA layer effectively prevented the aggregation of noble metal NPs in water–alcohol mixed solutions and provided chemical affinity to silica. A high degree of monodispersity and homogeneous shell thickness of the coatings were readily obtained, and were characterized by FE-SEM images and absorption spectra. This new method can be applied to a broad range of nanocolloids onto which the thiol base can be adsorbed. The results of the synthesized metal@SiO_2@FITC NPs proved that the Au and Ag NPs could be used as plasmonic nanoantennas to enhance the fluorescence of FITC.

The biggest enhancement factors for $Ag@SiO_2$–FITC and $Au@SiO_2$–FITC were 4.21 and 2.07, respectively.

Acknowledgements

This work was supported by the National Natural Science Foundation of China (60971026, 11074249, 11004188, 61275197), an exchange program between CAS of China and KNAW of the Netherlands, the IOP program of the Netherlands and the John van Geuns foundation.

References

1 S. Song, R. Liu, Y. Zhang, J. Feng, D. Liu, Y. Xing, F. Zhao and H. J. Zhang, *Chem.–Eur. J.*, 2010, **16**, 6251–6256.
2 W. L. Barnes, A. Dereux and T. W. Ebbesen, *Nature*, 2003, **424**, 824–830.
3 R. Elghanjan, J. J. Storhoff, R. C. Mucic, R. L. Letsinger and C. A. Mirkin, *Science*, 1997, **277**, 1078–1080.
4 W. C. Law, K. T. Yong, A. Baev and P. N. Prasad, *ACS Nano*, 2011, **5**, 4858–4864.
5 R. L. Stoermer, K. B. Cederquist, S. K. McFarland, M. Y. Sha, S. G. Penn and C. D. Keating, *J. Am. Chem. Soc.*, 2006, **128**, 16892–16903.
6 A. Guerrero-Martinez, J. Perez-Juste and L. M. Liz-Marzán, *Adv. Mater.*, 2010, **22**, 1182–1195.
7 L. Levy, Y. Sahoo, K. S. Kim, E. J. Bergey and P. N. Prasad, *Chem. Mater.*, 2002, **14**, 3715–3721.
8 D. Cheng and Q. H. Xu, *Chem. Commun.*, 2007, 248–250.
9 N. Liu, B. S. Prall and V. I. Klimov, *J. Am. Chem. Soc.*, 2006, **128**, 15362–15363.
10 J. Malicka, I. Gryczynski, J. Fang, J. Kusba and J. R. Lakowicz, *Anal. Biochem.*, 2003, **315**, 160.
11 S. Liu and M. Y. Han, *Chem.–Asian J.*, 2010, **5**, 36–45.
12 L. M. Liz-Marzán, M. Giersig and P. Mulvaney, *Langmuir*, 1996, **12**, 4329–4335.
13 V. V. Hardikar and E. Matijevic, *J. Colloid Interface Sci.*, 2000, **221**, 133–136.
14 C. Graf, D. L. J. Vossen, A. Imhof and A. Blaaderen, *Langmuir*, 2003, **19**, 6693–6700.
15 K. Landfester, *Angew. Chem., Int. Ed.*, 2009, **48**, 4488–4507.
16 I. Pastoriza-Santos, J. Prez-Juste and L. M. Liz-Marzán, *Chem. Mater.*, 2006, **18**, 2465–2467.
17 S. M. Kang, K. B. Lee, D. J. Kim and J. S. Choi, *Nanotechnology*, 2006, **17**, 4719–4725.
18 S. H. Liu, Z. H. Zhang and M. Y. Han, *Adv. Mater.*, 2005, **17**, 1862–1866.
19 S. H. Liu and M. Y. Han, *Adv. Funct. Mater.*, 2005, **15**, 961–967.
20 Y. Lu, Y. D. Yin, Z. Y. Li and Y. N. Xia, *Nano Lett.*, 2002, **2**, 785–788.
21 W. Stober, A. Fink and E. Bohn, *J. Colloid Interface Sci.*, 1968, **26**, 62–69.
22 R. Shen, P. H. Camargo, Y. N. Xia and H. Yang, *Langmuir*, 2008, **24**, 11189–11195.
23 C. D. Bain, E. B. Troughton, Y. T. Tao, J. Evall, G. M. Whiteside and R. G. Nuzo, *J. Am. Chem. Soc.*, 1989, **111**, 321–335.
24 Y. Y. Zhao, Z. Wang and X. Y. Jiang, *Nanoscale*, 2010, **2**, 2114–2119.
25 Y. Kim, R. C. Johnson and J. T. Hupp, *Nano Lett.*, 2001, **1**, 165–167.
26 M. Ortiz, A. Fragoso and C. K. O'Sullivan, *Anal. Chem.*, 2011, **83**, 2931–2938.
27 D. Joseph and K. E. Gekeler, *Langmuir*, 2009, **25**, 13224–13231.
28 G. C. Herdt, D. R. Jung and A. W. Czanderna, *Prog. Surf. Sci.*, 1995, **50**, 103–129.
29 H. Hiramatsu and F. E. Osterloh, *Chem. Mater.*, 2004, **16**, 2509–2511.
30 C. Fernandez-Lopez, C. Mateo-Mateo, R. A. Alvrez-Puebla, J. Perez-Juste, I. Pastoriza-Santos and L. M. Liz-Marzán, *Langmuir*, 2009, **25**, 13894–13899.
31 S. Pierrat, I. Zins, A. Breivogen and C. Sonnichsen, *Nano Lett.*, 2007, **7**, 259–263.
32 M. Ming, Y. Chen and A. Katz, *Langmuir*, 2002, **18**, 8566–8572.
33 A. F. Wallace, J. J. DeYoreo and P. M. Dove, *J. Am. Chem. Soc.*, 2009, **131**, 5244–5250.
34 N. R. Jana, L. Gearheart and C. J. Murphy, *Langmuir*, 2001, **17**, 6782–6786.
35 Q. H. Zeng, Y. L. Zhang, X. M. Liu, L. P. Tu, X. G. Kong and H. Zhang, *Chem. Commun.*, 2012, **48**, 1781–1783.
36 K. Aslan and V. H. Perez-Luna, *Langmuir*, 2002, **18**, 6059–6065.
37 P. Galletto, P. F. Brevet, H. H. Girault, R. Antoine and M. Broyer, *J. Phys. Chem. B*, 1999, **103**, 8706–8710.
38 J. Liao, Y. Zhang, W. Yu, L. Xu, C. Ge, J. Liu and N. Gu, *Colloids Surf., A*, 2003, **223**, 177–183.
39 K. L. Kelly, E. Coronado, L. L. Zhao and G. C. Schatz, *J. Phys. Chem. B*, 2003, **107**, 668–677.
40 X. H. Huang, S. Neretina and M. A. El-Sayed, *Adv. Mater.*, 2009, **21**, 1–31.
41 A. D. McFarland and R. P. Van Duyne, *Nano Lett.*, 2003, **3**, 1057–1062.
42 X. Dong, X. Ji, H. Wu, L. Zhao, J. Li and W. Yang, *J. Phys. Chem. C*, 2009, **113**, 6573–6576.
43 C. Xue, X. Chen, S. J. Hurst and C. A. Mirkin, *Adv. Mater.*, 2007, **19**, 4071–4074.
44 B. P. Bastakoti, S. Guragain, S. Yusa and K. Nakashima, *RSC Adv.*, 2012, **2**, 5938–5940.